Crystal structure, Hirshfeld surface analysis and interaction energy and DFT studies of (S)-10-propargyl-pyrrolo[2,1-c][1,4]benzodiazepine-5,11-dione

Dounia Jeroundi, Ahmed Mazzah, Tuncer Hokelek, El Mestafa El Hadrami, Catherine Renard, Amal Haoudi, El Mokhtar Essassi

▶ **To cite this version:**

Dounia Jeroundi, Ahmed Mazzah, Tuncer Hokelek, El Mestafa El Hadrami, Catherine Renard, et al.. Crystal structure, Hirshfeld surface analysis and interaction energy and DFT studies of (S)-10-propargylpyrrolo[2,1-c][1,4]benzodiazepine-5,11-dione. Acta crystallographica Section E : Crystallographic communications [2015-..], 2020, 76, pp.467-472. 10.1107/S2056989020002698 . hal-04438460

HAL Id: hal-04438460
https://hal.univ-lille.fr/hal-04438460

Submitted on 5 Feb 2024

HAL is a multi-disciplinary open access archive for the deposit and dissemination of scientific research documents, whether they are published or not. The documents may come from teaching and research institutions in France or abroad, or from public or private research centers.

L'archive ouverte pluridisciplinaire **HAL**, est destinée au dépôt et à la diffusion de documents scientifiques de niveau recherche, publiés ou non, émanant des établissements d'enseignement et de recherche français ou étrangers, des laboratoires publics ou privés.

Acta Cryst E CRYSTALLOGRAPHIC COMMUNICATIONS

ISSN 2056-9890

Crystal structure, Hirshfeld surface analysis and interaction energy and DFT studies of (*S*)-10-propargylpyrrolo[2,1-*c*][1,4]benzodiazepine-5,11-dione

Dounia Jeroundi,[a]* Ahmed Mazzah,[b] Tuncer Hökelek,[c] El Mestafa El Hadrami,[a] Catherine Renard,[d] Amal Haoudi[a] and El Mokhtar Essassi[e]

[a]Laboratory of Applied Organic Chemistry, Sidi Mohamed Ben Abdellah University, Faculty of Sciences and Techniques, Road Immouzer, BP 2202 Fez, Morocco, [b]USR 3290 Miniaturisation pour l'analyse, la synthèse et la protéomique, 59655, Villeneuve d'Ascq Cedex, Université Lille1, France, [c]Department of Physics, Hacettepe University, 06800 Beytepe, Ankara, Turkey, [d]Unité de Catalyse et de Chimie du Solide (UCCS), UMR 8181, Ecole Nationale Supérieure de Chimie de Lille, Université Lille 1, 59650 Villeneuve d'Ascq Cedex, France, and [e]Laboratoire de Chimie Organique Hétérocyclique URAC 21, Pôle de Compétence Pharmacochimie, Av. Ibn Battouta, BP 1014, Faculté des Sciences, Université Mohammed V, Rabat, Morocco. *Correspondence e-mail: DouniaJeroundi2019@gmail.com

Received 27 January 2020
Accepted 26 February 2020

Edited by A. J. Lough, University of Toronto, Canada

Keywords: crystal structure; benzodiazepine; pyrrole; Hirshfeld surface.

CCDC reference: 1986475

Supporting information: this article has supporting information at journals.iucr.org/e

The title compound, $C_{15}H_{14}N_2O_2$, consists of pyrrole and benzodiazepine units linked to a propargyl moiety, where the pyrrole and diazepine rings adopt half-chair and boat conformations, respectively. The absolute configuration was assigned on the the basis of L-proline, which was used in the synthesis of benzodiazepine. In the crystal, weak $C-H_{Bnz}\cdots O_{Diazp}$ and $C-H_{Proprg}\cdots O_{Diazp}$ (Bnz = benzene, Diazp = diazepine and Proprg = propargyl) hydrogen bonds link the molecules into two-dimensional networks parallel to the *bc* plane, enclosing $R_4^4(28)$ ring motifs, with the networks forming oblique stacks along the *a*-axis direction. The Hirshfeld surface analysis of the crystal structure indicates that the most important contributions for the crystal packing are from H···H (49.8%), H···C/C···H (25.7%) and H···O/O···H (20.1%) interactions. Hydrogen bonding and van der Waals interactions are the dominant interactions in the crystal packing. Computational chemistry indicates that in the crystal, C—H···O hydrogen-bond energies are 38.8 (for $C-H_{Bnz}\cdots O_{Diazp}$) and 27.1 (for $C-H_{Proprg}\cdots O_{Diazp}$) kJ mol^{-1}. Density functional theory (DFT) optimized structures at the B3LYP/6–311 G(d,p) level are compared with the experimentally determined molecular structure in the solid state. The HOMO–LUMO behaviour was elucidated to determine the energy gap.

1. Chemical context

Over the past few decades, compounds bearing heterocyclic nuclei have received much attention of chemists and biologists because of their importance in the development of chemotherapeutic agents and a wide variety of drugs (Cargill *et al.*, 1974; Micale *et al.*, 2004; Hadac *et al.*, 2006; Ourahou *et al.*, 2011). 1,4-Benzodiazepines and their derivatives have attracted the attention of chemists since the early 1960s, mainly because of the broad spectrum of biological properties exhibited by this class of compounds, in particular their psychopharmacological properties (Thurston & Langley, 1986; Kamal *et al.*, 2007; Antonow *et al.*, 2007; Archer & Sternbach, 1968; Mohiuddin *et al.*, 1986, Bose *et al.*, 1992; Gregson *et al.*, 2004). The vast commercial success of these medicinal agents has resulted in their chemistry being a major focus of research in the field of medicinal chemistry and many such ring systems having been described (Benzeid *et al.*, 2009*a*,*b*; Randles &

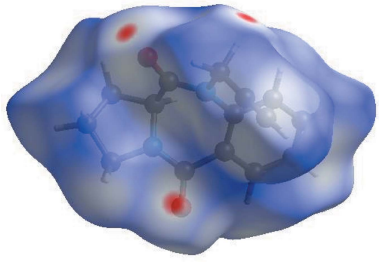

OPEN ACCESS

Storr, 1984; Sugasawa *et al.*, 1985; Cipolla *et al.*, 2009). Pyrrolo[2,1-*c*][1,4]benzodiazepines are a group of potent chemicals produced by Streptomyces species. For their anti-cancer activity, see: Bose *et al.* (1992); Cargill *et al.* (1974); Gregson *et al.* (2004).

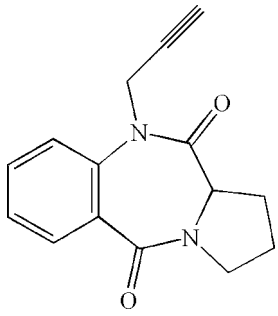

In a continuation of our research work on the advancement of benzodiazepine derivatives, we have developed a new synthethis for 10-propargylpyrrolo[2,1-*c*][1,4]benzodiazepine-5,11-dione (Fig. 1) in good yield from pyrrolo[2,1-*c*][1,4]-benzodiazepine with propargylbromide in the presence of tetra-*n*-butylammonium bromide (TBAB) as catalyst and potassium carbonate as base (Makosza & Jonczyk, 1976). The synthesized compound was characterized by single-crystal X-ray diffraction as well as Hirshfeld surface analysis. The results of the calculations by density functional theory (DFT), carried out at the B3LYP/6-311G (d,p) level, are compared with the experimentally determined molecular structure in the solid state.

2. Structural commentary

The title compound, (I), consists of pyrrole and benzodiazepine units linked to a propargyl moiety (Fig. 1). The five-membered pyrrole ring (N1/C8/C10–C12) adopts a half-chair conformation [puckering parameters q_2 = 0.376 (3) Å and θ = 94.4 (4)°] while the seven-membered diazepine ring (N1/N2/C1/C6–C9) adopts a boat conformation [Q_T = 0.9262 (13), q_2 = 0.9070 (14), q_3 = 0.1875 (16) Å, φ_2 = 105.6 (4) and φ = 161.4 (5)°]. In the propargyl moiety, the N2—C13—C14 and C13—C14—C15 bond angles are 112.66 (17)° and 177.4 (3)°, respectively.

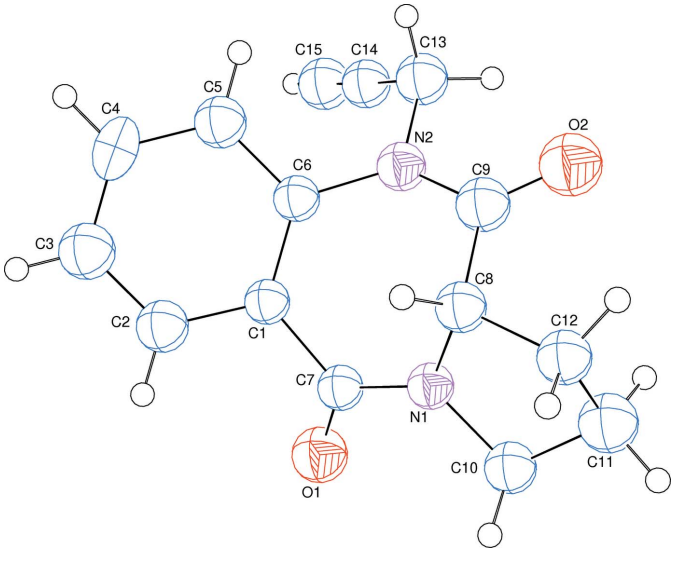

Figure 1
The molecular structure of the title compound with the atom-numbering scheme. Displacement ellipsoids are drawn at the 50% probability level.

Table 1
Hydrogen-bond geometry (Å, °).

D—H···A	D—H	H···A	D···A	D—H···A
C2—H2···O2^{vii}	0.93	2.53	3.252 (2)	135
C13—H13A···O1^{viii}	0.97	2.54	3.395 (3)	147

Symmetry codes: (vii) $x, y, z+1$; (viii) $-x+1, y-\frac{1}{2}, -z+1$.

3. Supramolecular features

In the crystal, weak C—H_{Bnz}···O_{Diazp} and C—H_{Proprg}···O_{Diazp} (Bnz = benzene, Diazp = diazepine and Proprg = propargyl) hydrogen bonds (Table 1) link the molecules into two-dimensional networks parallel to the *bc* plane, enclosing $R_4^4(28)$ ring motifs (Fig. 2), with the networks forming oblique stacks along the *a*-axis direction.

4. Hirshfeld surface analysis

In order to visualize the intermolecular interactions in the crystal of the title compound, a Hirshfeld surface (HS) analysis (Hirshfeld, 1977; Spackman & Jayatilaka, 2009) was carried out using *Crystal Explorer 17.5* (Turner *et al.*, 2017). In the HS plotted over d_{norm} (Fig. 3), the white surface indicates contacts with distances equal to the sum of van der Waals radii, and the red and blue colours indicate distances shorter (in close contact) or longer (distinct contact) than the van der Waals radii, respectively (Venkatesan *et al.*, 2016). The bright-

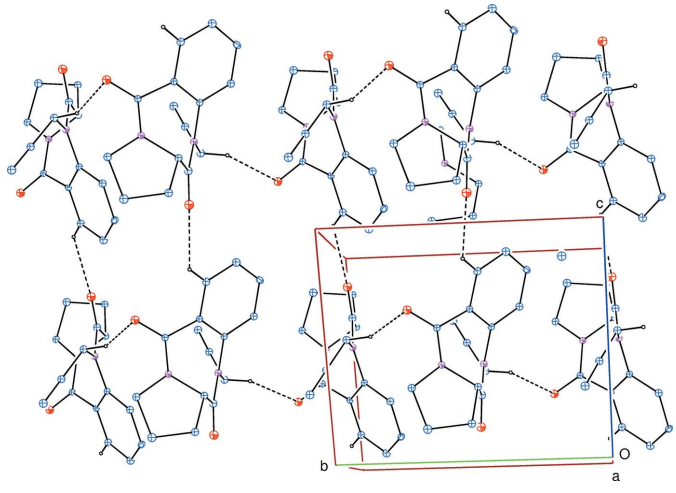

Figure 2
A partial packing diagram viewed along the *a*-axis direction with weak intermolecular C—H_{Bnz}···O_{Diazp} and C—H_{Proprg}···O_{Diazp} (Bnz = benzene, Diazp = diazepine and Proprg = propargyl) hydrogen bonds (dashed lines). H atoms not included in hydrogen bonding have been omitted for clarity.

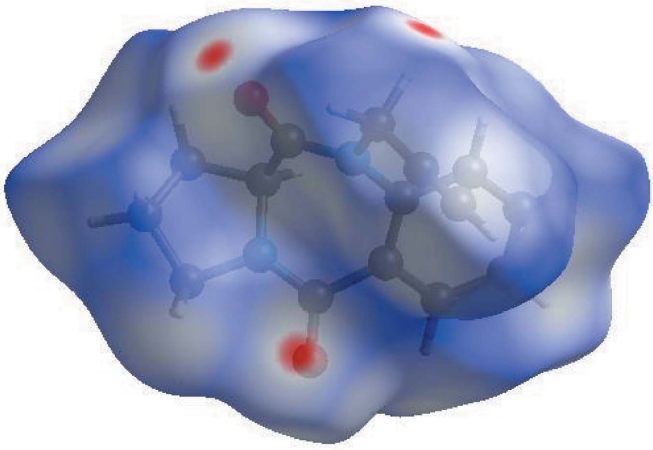

Figure 3
View of the three-dimensional Hirshfeld surface of the title compound plotted over d_{norm} in the range −0.1285 to 1.4451 a.u.

red spots appearing near O1, O2 and hydrogen atom H13*A* indicate their roles as the respective donors and acceptors; they also appear as blue and red regions corresponding to positive and negative potentials on the HS mapped over electrostatic potential (Spackman *et al.*, 2008; Jayatilaka *et al.*, 2005) shown in Fig. 4. Here the blue regions indicate positive electrostatic potential (hydrogen-bond donors), while the red regions indicate negative electrostatic potential (hydrogen-bond acceptors). The shape-index of the HS is a tool to visualize the π–π stacking by the presence of adjacent red and blue triangles; if there are no adjacent red and/or blue triangles, then there are no π–π interactions. Fig. 5 clearly suggests that there are no π–π interactions in (I).

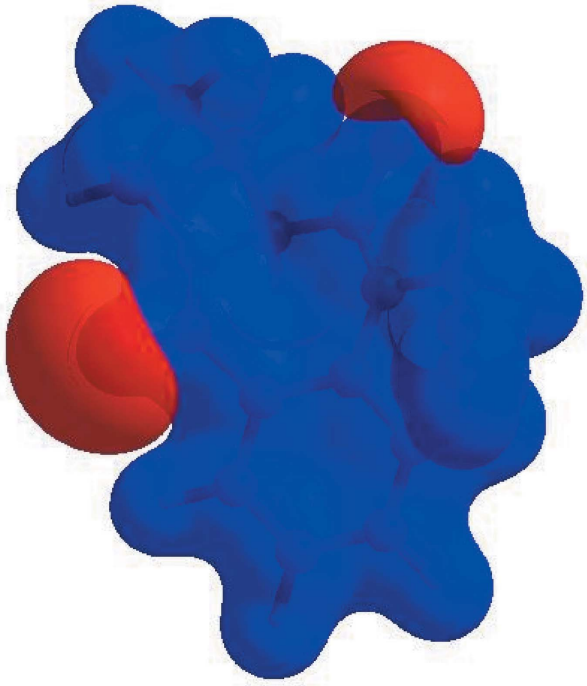

Figure 4
View of the three-dimensional Hirshfeld surface of the title compound plotted over electrostatic potential energy in the range −0.0500 to 0.0500 a.u. using the STO-3 G basis set at the Hartree–Fock level of theory. Hydrogen-bond donors and acceptors are shown as blue and red regions around the atoms, corresponding to positive and negative potentials, respectively.

Table 2
Selected interatomic distances (Å).

O1···C15^{i}	3.273 (4)	O2···H4^{ii}	2.69
O1···C13^{ii}	3.395 (3)	N1···N2	2.898 (2)
O2···C2^{iii}	3.252 (2)	C2···C10^{v}	3.558 (3)
O2···C11	3.303 (3)	C4···C12^{vi}	3.552 (4)
O2···C4^{ii}	3.397 (3)	C5···C14	3.090 (4)
O1···H8^{iv}	2.82	C7···C15^{i}	3.512 (4)
O1···H12*A*^{iv}	2.76	C1···H8	2.69
O1···H2	2.63	C3···H12*A*^{vi}	2.90
O1···H10*A*	2.73	C3···H11*B*^{v}	2.87
O1···H15^{i}	2.81	C5···H13*A*	2.86
O1···H13*A*^{ii}	2.54	C6···H8	2.69
O2···H2^{iii}	2.53	C7···H13*A*^{ii}	2.93
O2···H12*B*	2.45	C13···H5	2.66
O2···H13*B*	2.32	C14···H5	2.92
O2···H11*A*	2.89	H5···H13*A*	2.32

Symmetry codes: (i) $x-1, y, z$; (ii) $-x+1, y+\frac{1}{2}, -z+1$; (iii) $x, y, z-1$; (iv) $-x, y+\frac{1}{2}, -z+1$; (v) $-x, y-\frac{1}{2}, -z+1$; (vi) $x+1, y, z+1$.

The overall two-dimensional fingerprint plot, Fig. 6*a*, and those delineated into H···H, H···C/C···H, H···O/O···H, C···C and H···N/N···H contacts (McKinnon *et al.*, 2007) are illustrated in Fig. 6 *b*–*f*, respectively, together with their relative contributions to the Hirshfeld surface. The most important interaction is H···H contributing 49.8% to the overall crystal packing, which is reflected in Fig. 6*b* as widely scattered points of high density due to the large hydrogen content of the molecule with the tip at $d_e = d_i = 1.13$ Å. In the absence of C—H $\cdots$ π interactions, the pairs of characteristic wings in Fig. 6*c* arises from H···C/C···H contacts (25.7% contribution to the HS); the pair of spikes have tips at $d_e + d_i = 2.80$ Å. The thin and thick pairs of scattered points of wings in the fingerprint plot delineated into H···O/O···H contacts (Fig. 6*d*, 20.1%) have a symmetrical distribution of points with the edges at $d_e + d_i = 2.42$ and 2.44 Å, respectively. The C···C contacts (Fig. 6*e*, 1.8%) have a pliers-shaped distribution of points with the tips at $d_e + d_i = 3.47$ Å. Finally, the H $\cdots$ N/N···H interactions

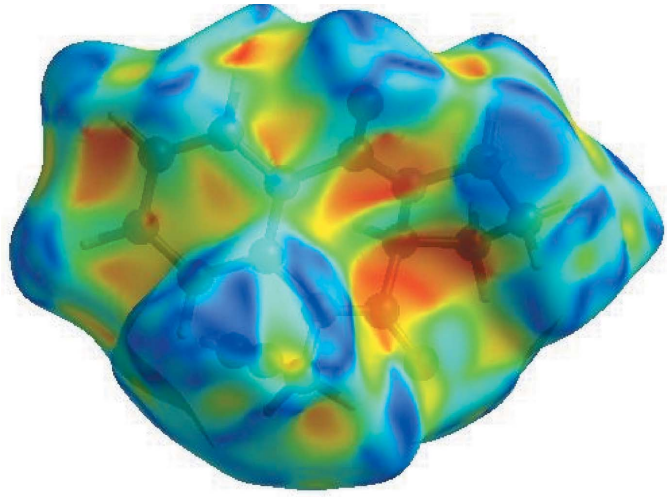

Figure 5
Hirshfeld surface of the title compound plotted over shape-index.

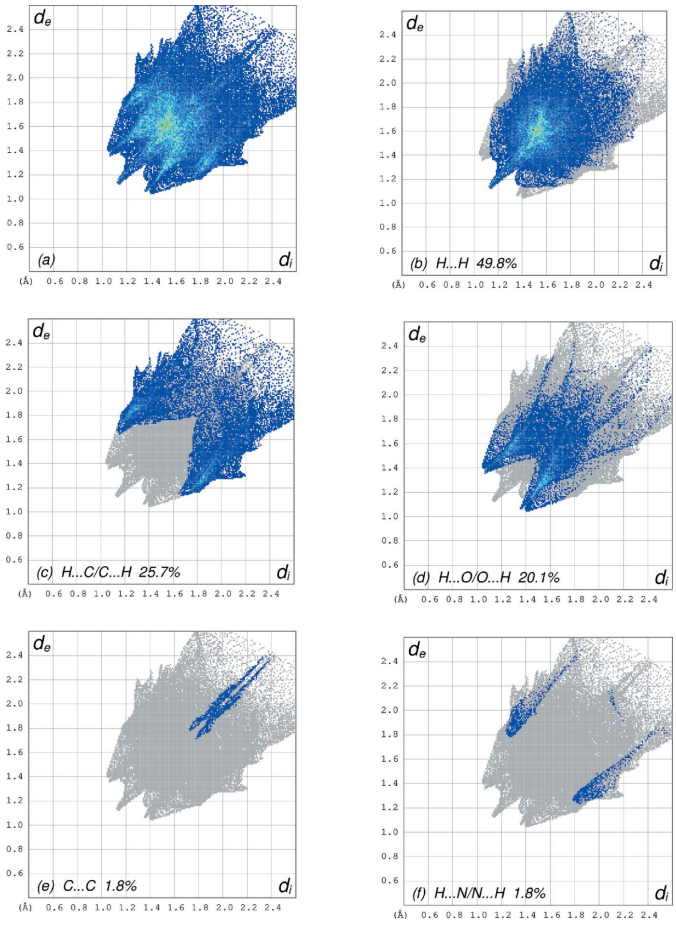

Figure 6
The full two-dimensional fingerprint plots for the title compound, showing (*a*) all interactions, and delineated into (*b*) H···H, (*c*) H···C/C···H, (*d*) H···O/O···H, (*e*) C···C and (*f*) H···N/N···H interactions. The d_i and d_e values are the closest internal and external distances (in Å) from given points on the Hirshfeld surface contacts.

(1.8%) are reflected in Fig. 6*f* as thick wings with the tips at $d_e + d_i$ = 3.04 Å. Selected contacts are listed in Table 2.

The Hirshfeld surface representations with the function d_{norm} plotted onto the surface are shown for the H···H, H···C/C···H and H···O/O···H interactions in Fig. 7*a–c*, respectively.

The Hirshfeld surface analysis confirms the importance of H-atom contacts in establishing the packing. The large number of H···H, H···C/C···H and H···O/O···H interactions suggest that van der Waals interactions and hydrogen bonding play the major roles in the crystal packing (Hathwar *et al.*, 2015).

5. Interaction energy calculations

The intermolecular interaction energies were calculated using the CE–B3LYP/6–31G(d,p) energy model in *Crystal Explorer 17.5* (Turner *et al.*, 2017), where a cluster of molecules is generated by applying crystallographic symmetry operations with respect to a selected central molecule within a default radius of 3.8 Å (Turner *et al.*, 2014). The total intermolecular energy (E_{tot}) is the sum of electrostatic (E_{ele}), polarization (E_{pol}), dispersion (E_{dis}) and exchange-repulsion (E_{rep}) energies (Turner *et al.*, 2015) with scale factors of 1.057, 0.740, 0.871 and 0.618, respectively (Mackenzie *et al.*, 2017). Hydrogen-bonding interaction energies (in kJ mol^{-1}) were calculated as −13.2 (E_{ele}), −3.8 (E_{pol}), −45.1 (E_{dis}), 27.8 (E_{rep}) and −38.8 (E_{tot}) for C2—H2···O2 and −10.7 (E_{ele}), −4.0 (E_{pol}), −25.8 (E_{dis}), 15.7 (E_{rep}) and −27.1 (E_{tot}) for C13—H13*A*···O1.

Table 3
Comparison of the selected (X-ray and DFT) geometric data (Å, °).

Bonds/angles	X-ray	B3LYP/6–311G(d,p)
O1—C7	1.231 (2)	1.30064
O2—C9	1.222 (2)	1.30459
N1—C7	1.337 (2)	1.44900
N1—C8	1.474 (2)	1.42892
N1—C10	1.476 (2)	1.41852
N2—C6	1.429 (2)	1.45461
N2—C9	1.362 (2)	1.45679
N2—C13	1.478 (2)	1.48990
C7—N1—C8	124.64 (14)	125.54242
C7—N1—C10	122.81 (16)	120.48706
C8—N1—C10	112.28 (14)	111.27162
C6—N2—C13	118.67 (14)	116.39016
C9—N2—C6	123.48 (14)	122.08303
C9—N2—C13	116.98 (15)	113.69042
C1—C6—N2	122.46 (14)	120.60573
C5—C6—N2	118.13 (15)	117.33963

6. DFT calculations

The optimized structure of the title compound in the gas phase was generated theoretically *via* density functional theory (DFT) using standard B3LYP functional and 6–311 G(d,p) basis-set calculations (Becke, 1993) as implemented in *GAUSSIAN 09* (Frisch *et al.*, 2009). The theoretical and experimental results were in good agreement (Table 3). The

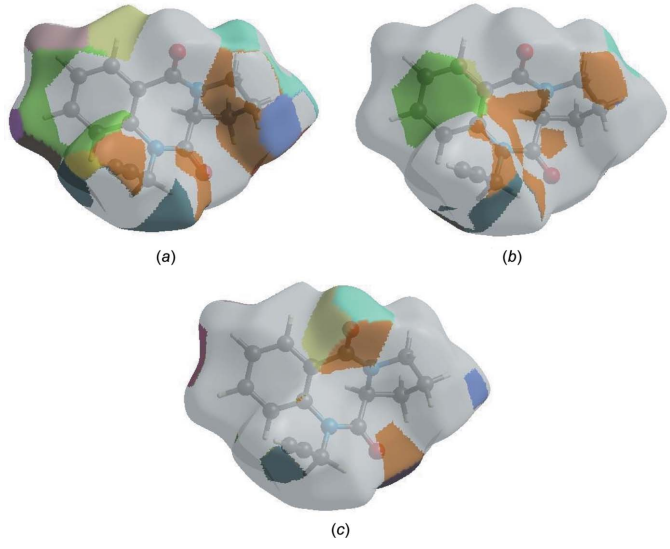

Figure 7
Hirshfeld surface representations with the function d_{norm} plotted onto the surface for (*a*) H···H, (*b*) H···C/C···H and (*c*) H···O/O···H interactions.

Table 4
Calculated energies.

Molecular Energy (a.u.) (eV)	Compound (I)
Total Energy, *TE* (eV)	−22499
E_{HOMO} (eV)	−4.0030
E_{LUMO} (eV)	−0.5203
Gap ΔE (eV)	3.4829
Dipole moment, μ (Debye)	2.2189
Ionization potential, *I* (eV)	4.0030
Electron affinity, *A*	0.5203
Electronegativity, χ	2.2617
Hardness, η	1.7414
Electrophilicity index, ω	1.4687
Softness, σ	0.5742
Fraction of electron transferred, ΔN	1.3605

highest-occupied molecular orbital (HOMO), acting as an electron donor, and the lowest-unoccupied molecular orbital (LUMO), acting as an electron acceptor, are very important parameters for quantum chemistry. When the energy gap is small, the molecule is highly polarizable and has high chemical reactivity. The DFT calculations provide some important information on the reactivity and site selectivity of the molecular framework. E_{HOMO} and E_{LUMO} clarify the inevitable charge-exchange collaboration inside the studied material, and are given in Table 4 along with the electronegativity (χ), hardness (η), potential (μ), electrophilicity (ω) and softness (σ). The significance of η and σ is to evaluate both the reactivity and stability. The electron transition from the HOMO to the LUMO energy level is shown in Fig. 8. The HOMO and

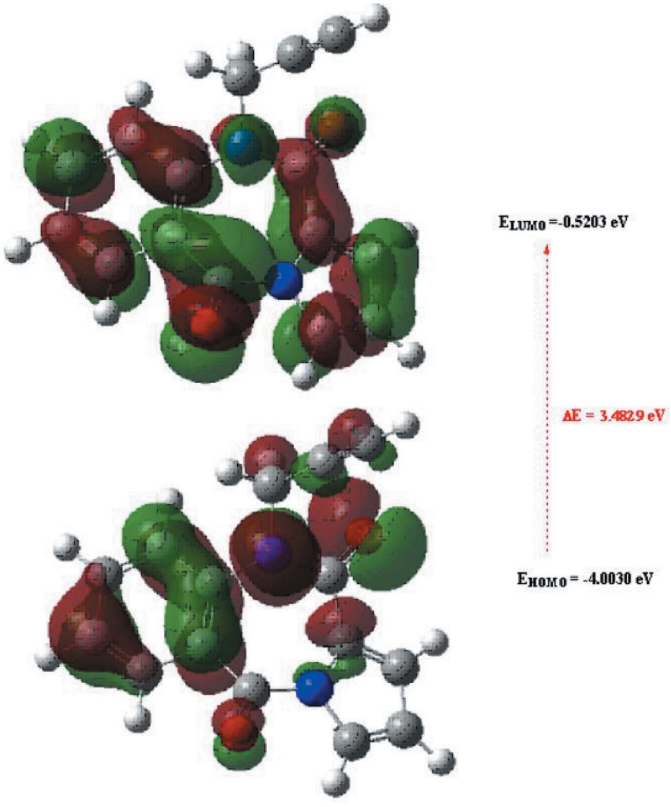

Figure 8
The energy band gap of the title compound.

Table 5
Experimental details.

Crystal data	
Chemical formula	$C_{15}H_{14}N_2O_2$
M_r	254.28
Crystal system, space group	Monoclinic, $P2_1$
Temperature (K)	299
a, *b*, *c* (Å)	8.4959 (2), 9.6479 (2), 8.7619 (2)
β (°)	116.921 (1)
V (Å^3)	640.36 (3)
Z	2
Radiation type	Mo $K\alpha$
μ (mm^{-1})	0.09
Crystal size (mm)	0.39 × 0.37 × 0.16
Data collection	
Diffractometer	Bruker APEXII CCD
Absorption correction	Multi-scan (*SADABS*; Bruker, 2013)
T_{min}, T_{max}	0.684, 0.746
No. of measured, independent and observed [$I > 2\sigma(I)$] reflections	12206, 3821, 3349
R_{int}	0.024
(sin $\theta/\lambda)_{max}$ (Å^{-1})	0.714
Refinement	
$R[F^2 > 2\sigma(F^2)]$, $wR(F^2)$, *S*	0.039, 0.103, 1.06
No. of reflections	3821
No. of parameters	172
No. of restraints	1
H-atom treatment	H-atom parameters constrained
$\Delta\rho_{max}$, $\Delta\rho_{min}$ (e Å^{-3})	0.20, −0.15
Absolute structure	Flack *x* determined using 1347 quotients $[(I^+)-(I^-)]/[(I^+)+(I^-)]$ (Parsons *et al.*, 2013)
Absolute structure parameter	−0.4 (3)

Computer programs: *APEX3* and *SAINT* (Bruker, 2013), *SHELXT* (Sheldrick, 2015*a*), *SHELXL* (Sheldrick, 2015*b*) and *OLEX2* (Dolomanov *et al.*, 2009).

LUMO are localized in the plane extending from the whole 10-propargylpyrrolo[2,1-*c*][1,4]benzodiazepine-5,11-dione ring. The energy band gap [$\Delta E = E_{LUMO} - E_{HOMO}$] of the molecule is 3.4829 eV, and the frontier molecular orbital energies, E_{HOMO} and E_{LUMO} are −4.0030 and −0.5203 eV, respectively.

7. Database survey

A alkylated analogue has been reported, *viz*. 10-allyl-2,3-dihydro-1*H*-pyrrolo[2,1-*c*][1,4]benzodiazepine-5,11(10*H*,11a*H*)-dione (Benzeid *et al.*, 2009*a*), as well as three similar structures, 2-hydroxy-10-propargylpyrrolo[2,1-*c*][1,4]benzodiazepine-5,11-dione monohydrate (Ourahou *et al.* 2010), *rac*-9,10-dimethoxy-3-methyl-6-phenyl-7,7adihydrobenzo[*b*]benzo-[4,5]isothiazolo[2,3-*d*][1,4]diazepine 12,12-dioxide (Bassin *et al.*, 2011) and (*S*)-2,3,5,10,11,11a-hexahydro-1*H*-pyrrolo-[2,1-*c*][1,4]benzodiazepine-3,11-dione (Cheng *et al.* 2007).

8. Synthesis and crystallization

The synthesis of pyrrolobenzodiazepine is a simple condensation of isatoic anhydride on L-proline. Pyrrolo[2,1-*c*][1,4]-benzodiazepine-5,11-dione (2.15 mmol), propargyl bromide (2.15 mmol) and potassium carbonate (4.3 mmol) along with a

catalytic amount of tetra-*n*-butyl ammonium bromide were stirred in *N*,*N*-dimethylformamide (20 ml) for 72 h. The solid material was removed by filtration and the solvent evaporated under vacuum. The residue was separated by chromatography on silica gel with an *n*-hexane–ethyl acetate (1:9) solvent system. The title compound was obtained as colourless crystals in 70% yield upon evaporation of the solvent.

9. Refinement

Crystal data, data collection and structure refinement details are summarized in Table 5. The C-bound H atoms were positioned geometrically, with C—H = 0.93 Å (for aromatic and propagyl moiety's H atoms), 0.98 Å (for methine H atom) and 0.97 Å (for methylene H atoms), and constrained to ride on their parent atoms, with U_{iso}(H) = 1.U_{eq}(C).

Funding information

TH is grateful to Hacettepe University Scientific Research Project Unit (grant No. 013 D04 602 004).

References

Antonow, D., Jenkins, T. C., Howard, P. W. & Thurston, D. E. (2007). *Bioorg. Med. Chem.* **15**, 3041–3053.
Archer, G. A. & Sternbach, L. H. (1968). *Chem. Rev.* **68**, 747–784.
Bassin, J. P., Shah, V. P., Martin, L. & Horton, P. N. (2011). *Acta Cryst.* E**67**, o684–o685.
Becke, A. D. (1993). *J. Chem. Phys.* **98**, 5648–5652.
Benzeid, H., Essassi, E. M., Saffon, N., Garrigues, B. & Ng, S. W. (2009*a*). *Acta Cryst.* E**65**, o2322.
Benzeid, H., Saffon, N., Garrigues, B., Essassi, E. M. & Ng, S. W. (2009*b*). *Acta Cryst.* E**65**, o2684.
Bose, D. S., Thompson, A. S., Ching, J. A., Hartley, J. A., Berardini, M. D., Jenkins, T. C., Neidle, S., Hurley, L. H. & Thurston, D. E. (1992). *J. Am. Chem. Soc.* **114**, 4939–4941.
Bruker (2013). *APEX3*, *SAINT* and *SADABS*. Bruker AXS, Inc., Madison, Wisconsin, USA.
Cargill, C., Bachmann, E. & Zbinden, G. (1974). *J. Natl Cancer Inst.* **53**, 481–486.
Cheng, M.-S., Ma, C., Liu, J.-H., Sha, Y. & Wang, Q.-H. (2007). *Acta Cryst.* E**63**, o4605.
Cipolla, L., Araújo, A. C., Airoldi, C. & Bini, D. (2009). *Anticancer Agents Med. Chem.* **9**, 1–31.
Dolomanov, O. V., Bourhis, L. J., Gildea, R. J., Howard, J. A. K. & Puschmann, H. (2009). *J. Appl. Cryst.* **42**, 339–341.
Frisch, M. J., *et al.* (2009). *GAUSSIAN09*. Gaussian Inc., Wallingford, CT, USA.
Gregson, S. T., Howard, P. W., Gullick, D. R., Hamaguchi, A., Corcoran, K. E., Brooks, N. A., Hartley, J. A., Jenkins, T. C., Patel, S., Guille, M. J. & Thurston, D. E. (2004). *J. Med. Chem.* **47**, 1161–1174.
Hadac, E. M., Dawson, E. S., Darrow, J. W., Sugg, E. E., Lybrand, T. P. & Miller, L. J. (2006). *J. Med. Chem.* **49**, 850–863.
Hathwar, V. R., Sist, M., Jørgensen, M. R. V., Mamakhel, A. H., Wang, X., Hoffmann, C. M., Sugimoto, K., Overgaard, J. & Iversen, B. B. (2015). *IUCrJ*, **2**, 563–574.
Hirshfeld, H. L. (1977). *Theor. Chim. Acta*, **44**, 129–138.
Jayatilaka, D., Grimwood, D. J., Lee, A., Lemay, A., Russel, A. J., Taylor, C., Wolff, S. K., Cassam-Chenai, P. & Whitton, A. (2005). *TONTO - A System for Computational Chemistry*. Available at: http://hirshfeldsurface.net/
Kamal, A., Reddy, K. L., Devaiah, V., Shankaraiah, N., Reddy, G. S. K. & Raghavan, S. (2007). *J. Comb. Chem.* **9**, 29–42.
Mackenzie, C. F., Spackman, P. R., Jayatilaka, D. & Spackman, M. A. (2017). *IUCrJ*, **4**, 575–587.
Makosza, M. & Jonczyk, A. (1976). *Org. Synth.* **55**, 91.
McKinnon, J. J., Jayatilaka, D. & Spackman, M. A. (2007). *Chem. Commun.* pp. 3814–3816.
Micale, N., Vairagoundar, R., Yakovlev, A. G. & Kozikowski, A. P. (2004). *J. Med. Chem.* **47**, 6455–6458.
Mohiuddin, C., Reddy, P. S., Ahmed, K. & Ratnam, C. V. (1986). *Heterocycles*, **24**, 3489–3530.
Ourahou, S., Chammache, M., Zouihri, H., Essassi, E. M. & Ng, S. W. (2010). *Acta Cryst.* E**66**, o731.
Ourahou, S., Zouihri, H., Massoui, M., Essassi, E. M. & Ng, S. W. (2011). *Acta Cryst.* E**67**, o1906.
Parsons, S., Flack, H. D. & Wagner, T. (2013). *Acta Cryst.* B**69**, 249–259.
Randles, K. R. & Storr, R. C. (1984). *J. Chem. Soc.* **22**, 1485–1486.
Sheldrick, G. M. (2015*a*). *Acta Cryst.* A**71**, 3–8.
Sheldrick, G. M. (2015*b*). *Acta Cryst.* C**71**, 3–8.
Spackman, M. A. & Jayatilaka, D. (2009). *CrystEngComm*, **11**, 19–32.
Spackman, M. A., McKinnon, J. J. & Jayatilaka, D. (2008). *CrystEngComm*, **10**, 377–388.
Sugasawa, T., Adachi, M., Sasakura, K., Matsushita, A., Eigyo, M., Shiomi, T., Shintaku, H., Takahara, Y. & Murata, S. (1985). *J. Med. Chem.* **28**, 699–707.
Thurston, D. E. & Langley, D. R. (1986). *J. Org. Chem.* **51**, 705–712.
Turner, M. J., Grabowsky, S., Jayatilaka, D. & Spackman, M. A. (2014). *J. Phys. Chem. Lett.* **5**, 4249–4255.
Turner, M. J., McKinnon, J. J., Wolff, S. K., Grimwood, D. J., Spackman, P. R., Jayatilaka, D. & Spackman, M. A. (2017). *CrystalExplorer17*. The University of Western Australia.
Turner, M. J., Thomas, S. P., Shi, M. W., Jayatilaka, D. & Spackman, M. A. (2015). *Chem. Commun.* **51**, 3735–3738.
Venkatesan, P., Thamotharan, S., Ilangovan, A., Liang, H. & Sundius, T. (2016). *Spectrochim. Acta Part A*, **153**, 625–636.

supporting information

Acta Cryst. (2020). E**76**, 467-472 [https://doi.org/10.1107/S2056989020002698]

Crystal structure, Hirshfeld surface analysis and interaction energy and DFT studies of (*S*)-10-propargylpyrrolo[2,1-*c*][1,4]benzodiazepine-5,11-dione

Dounia Jeroundi, Ahmed Mazzah, Tuncer Hökelek, El Mestafa El Hadrami, Catherine Renard, Amal Haoudi and El Mokhtar Essassi

Computing details

Data collection: *APEX3* (Bruker, 2013); cell refinement: *SAINT* (Bruker, 2013); data reduction: *SAINT* (Bruker, 2013); program(s) used to solve structure: SHELXT (Sheldrick, 2015a); program(s) used to refine structure: *SHELXL* (Sheldrick, 2015b); molecular graphics: *OLEX2* (Dolomanov *et al.*, 2009); software used to prepare material for publication: *OLEX2* (Dolomanov *et al.*, 2009).

(*S*)-10-(Prop-2-yn-1-yl)pyrrolo[2,1-*c*][1,4]benzodiazepine-5,11-dione

Crystal data

$C_{15}H_{14}N_2O_2$
$M_r = 254.28$
Monoclinic, $P2_1$
$a = 8.4959$ (2) Å
$b = 9.6479$ (2) Å
$c = 8.7619$ (2) Å
$\beta = 116.921$ (1)°
$V = 640.36$ (3) Å^3
$Z = 2$
$F(000) = 268$
$D_x = 1.319$ Mg m^{-3}
Mo $K\alpha$ radiation, $\lambda = 0.71073$ Å
Cell parameters from 6478 reflections
$\theta = 2.6$–28.5°
$\mu = 0.09$ mm^{-1}
$T = 299$ K
Plate, clear light colourless
0.39 × 0.37 × 0.16 mm

Data collection

Bruker APEXII CCD diffractometer
φ and ω scans
Absorption correction: multi-scan (SADABS; Bruker, 2013)
$T_{min} = 0.684$, $T_{max} = 0.746$
12206 measured reflections
3821 independent reflections
3349 reflections with $I > 2\sigma(I)$
$R_{int} = 0.024$
$\theta_{max} = 30.5°$, $\theta_{min} = 2.6°$
$h = -12 \rightarrow 12$
$k = -13 \rightarrow 13$
$l = -12 \rightarrow 12$

Refinement

Refinement on F^2
Least-squares matrix: full
$R[F^2 > 2\sigma(F^2)] = 0.039$
$wR(F^2) = 0.103$
$S = 1.06$
3821 reflections
172 parameters
1 restraint
Primary atom site location: dual
Hydrogen site location: inferred from neighbouring sites
H-atom parameters constrained
$w = 1/[\sigma^2(F_o^2) + (0.0554P)^2 + 0.0351P]$ where $P = (F_o^2 + 2F_c^2)/3$
$(\Delta/\sigma)_{max} < 0.001$
$\Delta\rho_{max} = 0.20$ e Å^{-3}
$\Delta\rho_{min} = -0.15$ e Å^{-3}

Absolute structure: Flack *x* determined using 1347 quotients $[(I^+)-(I^-)]/[(I^+)+(I^-)]$ (Parsons *et al.*, 2013)
Absolute structure parameter: −0.4 (3)

Special details

Geometry. All esds (except the esd in the dihedral angle between two l.s. planes) are estimated using the full covariance matrix. The cell esds are taken into account individually in the estimation of esds in distances, angles and torsion angles; correlations between esds in cell parameters are only used when they are defined by crystal symmetry. An approximate (isotropic) treatment of cell esds is used for estimating esds involving l.s. planes.

Fractional atomic coordinates and isotropic or equivalent isotropic displacement parameters (Å²)

	x	*y*	*z*	U_{iso}*/U_{eq}
O1	0.1993 (2)	0.71379 (15)	0.67243 (19)	0.0515 (4)
O2	0.2576 (2)	0.4767 (2)	0.15885 (17)	0.0621 (4)
N1	0.10489 (19)	0.59648 (15)	0.42473 (19)	0.0384 (3)
N2	0.41816 (19)	0.46005 (16)	0.44625 (18)	0.0389 (3)
C1	0.3344 (2)	0.49614 (17)	0.68011 (19)	0.0342 (3)
C2	0.3604 (2)	0.4606 (2)	0.8441 (2)	0.0441 (4)
H2	0.297976	0.507584	0.892040	0.053*
C3	0.4764 (3)	0.3576 (2)	0.9365 (2)	0.0518 (5)
H3	0.491032	0.334562	1.045179	0.062*
C4	0.5709 (3)	0.2888 (2)	0.8670 (3)	0.0525 (5)
H4	0.650555	0.219823	0.929588	0.063*
C5	0.5477 (3)	0.3218 (2)	0.7046 (3)	0.0466 (4)
H5	0.611399	0.274396	0.658401	0.056*
C6	0.4297 (2)	0.42536 (17)	0.6096 (2)	0.0347 (3)
C7	0.2084 (2)	0.61152 (17)	0.5927 (2)	0.0360 (3)
C8	0.0974 (2)	0.47097 (19)	0.3258 (2)	0.0383 (3)
H8	0.088877	0.387499	0.385319	0.046*
C9	0.2629 (2)	0.4673 (2)	0.3002 (2)	0.0396 (4)
C10	−0.0288 (3)	0.7001 (2)	0.3214 (3)	0.0540 (5)
H10A	0.021993	0.792198	0.337758	0.065*
H10B	−0.126879	0.701151	0.349469	0.065*
C11	−0.0863 (3)	0.6494 (3)	0.1404 (3)	0.0668 (7)
H11A	−0.009804	0.685371	0.094619	0.080*
H11B	−0.206984	0.676803	0.065910	0.080*
C12	−0.0705 (3)	0.4919 (3)	0.1595 (3)	0.0561 (5)
H12A	−0.171813	0.452660	0.167103	0.067*
H12B	−0.060151	0.449916	0.063901	0.067*
C13	0.5822 (3)	0.4646 (3)	0.4271 (3)	0.0522 (5)
H13A	0.618467	0.370691	0.419118	0.063*
H13B	0.558798	0.512036	0.321305	0.063*
C14	0.7252 (3)	0.5347 (3)	0.5684 (3)	0.0559 (5)
C15	0.8456 (4)	0.5887 (4)	0.6817 (4)	0.0771 (8)
H15	0.940820	0.631390	0.771234	0.092*

Atomic displacement parameters (Å²)

	U^{11}	U^{22}	U^{33}	U^{12}	U^{13}	U^{23}
O1	0.0594 (8)	0.0445 (7)	0.0560 (9)	−0.0014 (7)	0.0310 (7)	−0.0151 (6)
O2	0.0678 (9)	0.0904 (12)	0.0351 (7)	0.0028 (9)	0.0293 (6)	−0.0011 (8)
N1	0.0379 (7)	0.0392 (8)	0.0384 (8)	0.0031 (6)	0.0175 (6)	−0.0009 (6)
N2	0.0431 (7)	0.0439 (8)	0.0358 (7)	0.0055 (7)	0.0233 (6)	0.0027 (6)
C1	0.0366 (8)	0.0360 (8)	0.0303 (7)	−0.0079 (6)	0.0155 (6)	−0.0054 (6)
C2	0.0487 (9)	0.0538 (11)	0.0312 (8)	−0.0131 (9)	0.0191 (7)	−0.0088 (8)
C3	0.0566 (11)	0.0604 (12)	0.0291 (8)	−0.0183 (10)	0.0112 (8)	0.0028 (8)
C4	0.0526 (11)	0.0467 (11)	0.0432 (10)	−0.0022 (9)	0.0085 (9)	0.0108 (8)
C5	0.0476 (10)	0.0408 (10)	0.0479 (10)	0.0048 (8)	0.0186 (8)	0.0039 (8)
C6	0.0380 (8)	0.0349 (8)	0.0314 (8)	−0.0015 (6)	0.0160 (7)	0.0001 (6)
C7	0.0379 (8)	0.0362 (8)	0.0400 (9)	−0.0062 (6)	0.0230 (7)	−0.0055 (6)
C8	0.0425 (8)	0.0395 (8)	0.0326 (7)	−0.0066 (7)	0.0166 (6)	−0.0036 (7)
C9	0.0507 (9)	0.0383 (8)	0.0340 (8)	0.0012 (8)	0.0228 (7)	−0.0013 (7)
C10	0.0473 (10)	0.0560 (12)	0.0551 (12)	0.0131 (9)	0.0201 (9)	0.0082 (9)
C11	0.0597 (13)	0.0829 (17)	0.0490 (12)	0.0237 (13)	0.0169 (10)	0.0158 (12)
C12	0.0469 (10)	0.0737 (15)	0.0373 (9)	−0.0080 (10)	0.0099 (8)	−0.0042 (9)
C13	0.0510 (10)	0.0661 (13)	0.0520 (11)	0.0141 (10)	0.0343 (9)	0.0040 (10)
C14	0.0480 (11)	0.0657 (13)	0.0659 (14)	0.0053 (10)	0.0364 (11)	0.0103 (11)
C15	0.0588 (14)	0.093 (2)	0.0800 (19)	−0.0120 (14)	0.0319 (13)	0.0044 (15)

Geometric parameters (Å, º)

O1—C7	1.231 (2)	C5—C6	1.393 (2)
O2—C9	1.222 (2)	C8—H8	0.9800
N1—C7	1.337 (2)	C8—C9	1.521 (3)
N1—C8	1.474 (2)	C8—C12	1.522 (3)
N1—C10	1.476 (2)	C10—H10A	0.9700
N2—C6	1.429 (2)	C10—H10B	0.9700
N2—C9	1.362 (2)	C10—C11	1.513 (3)
N2—C13	1.478 (2)	C11—H11A	0.9700
C1—C2	1.394 (2)	C11—H11B	0.9700
C1—C6	1.399 (2)	C11—C12	1.527 (4)
C1—C7	1.493 (2)	C12—H12A	0.9700
C2—H2	0.9300	C12—H12B	0.9700
C2—C3	1.376 (3)	C13—H13A	0.9700
C3—H3	0.9300	C13—H13B	0.9700
C3—C4	1.378 (3)	C13—C14	1.450 (3)
C4—H4	0.9300	C14—C15	1.176 (4)
C4—C5	1.382 (3)	C15—H15	0.9300
C5—H5	0.9300		
O1···C15^{i}	3.273 (4)	O2···H4^{ii}	2.69
O1···C13^{ii}	3.395 (3)	N1···N2	2.898 (2)
O2···C2^{iii}	3.252 (2)	C2···C10^{v}	3.558 (3)
O2···C11	3.303 (3)	C4···C12^{vi}	3.552 (4)

O2···C4^{ii}	3.397 (3)	C5···C14	3.090 (4)
O1···H8^{iv}	2.82	C7···C15^{i}	3.512 (4)
O1···H12A^{iv}	2.76	C1···H8	2.69
O1···H2	2.63	C3···H12A^{vi}	2.90
O1···H10A	2.73	C3···H11B^{v}	2.87
O1···H15^{i}	2.81	C5···H13A	2.86
O1···H13A^{ii}	2.54	C6···H8	2.69
O2···H2^{iii}	2.53	C7···H13A^{ii}	2.93
O2···H12B	2.45	C13···H5	2.66
O2···H13B	2.32	C14···H5	2.92
O2···H11A	2.89	H5···H13A	2.32

C7—N1—C8	124.64 (14)	C9—C8—C12	112.98 (15)
C7—N1—C10	122.81 (16)	C12—C8—H8	110.8
C8—N1—C10	112.28 (14)	O2—C9—N2	122.16 (17)
C6—N2—C13	118.67 (14)	O2—C9—C8	122.34 (16)
C9—N2—C6	123.48 (14)	N2—C9—C8	115.42 (14)
C9—N2—C13	116.98 (15)	N1—C10—H10A	111.2
C2—C1—C6	118.81 (16)	N1—C10—H10B	111.2
C2—C1—C7	117.02 (15)	N1—C10—C11	102.59 (18)
C6—C1—C7	124.15 (14)	H10A—C10—H10B	109.2
C1—C2—H2	119.3	C11—C10—H10A	111.2
C3—C2—C1	121.41 (18)	C11—C10—H10B	111.2
C3—C2—H2	119.3	C10—C11—H11A	111.0
C2—C3—H3	120.2	C10—C11—H11B	111.0
C2—C3—C4	119.60 (18)	C10—C11—C12	103.65 (19)
C4—C3—H3	120.2	H11A—C11—H11B	109.0
C3—C4—H4	119.9	C12—C11—H11A	111.0
C3—C4—C5	120.23 (19)	C12—C11—H11B	111.0
C5—C4—H4	119.9	C8—C12—C11	103.60 (18)
C4—C5—H5	119.7	C8—C12—H12A	111.0
C4—C5—C6	120.63 (19)	C8—C12—H12B	111.0
C6—C5—H5	119.7	C11—C12—H12A	111.0
C1—C6—N2	122.46 (14)	C11—C12—H12B	111.0
C5—C6—N2	118.13 (15)	H12A—C12—H12B	109.0
C5—C6—C1	119.32 (15)	N2—C13—H13A	109.1
O1—C7—N1	122.16 (17)	N2—C13—H13B	109.1
O1—C7—C1	121.40 (16)	H13A—C13—H13B	107.8
N1—C7—C1	116.43 (14)	C14—C13—N2	112.66 (17)
N1—C8—H8	110.8	C14—C13—H13A	109.1
N1—C8—C9	108.01 (14)	C14—C13—H13B	109.1
N1—C8—C12	103.06 (16)	C15—C14—C13	177.4 (3)
C9—C8—H8	110.8	C14—C15—H15	180.0

Symmetry codes: (i) $x-1, y, z$; (ii) $-x+1, y+1/2, -z+1$; (iii) $x, y, z-1$; (iv) $-x, y+1/2, -z+1$; (v) $-x, y-1/2, -z+1$; (vi) $x+1, y, z+1$.

Hydrogen-bond geometry (Å, º)

D—H···*A*	*D*—H	H···*A*	*D*···*A*	*D*—H···*A*
C2—H2···O2^{vii}	0.93	2.53	3.252 (2)	135
C13—H13*A*···O1^{viii}	0.97	2.54	3.395 (3)	147

Symmetry codes: (vii) *x*, *y*, *z*+1; (viii) −*x*+1, *y*−1/2, −*z*+1.